ELSEVIER

Journal of Alloys and Compounds 388 (2005) 172–176

Journal of ALLOYS AND COMPOUNDS

www.elsevier.com/locate/jallcom

Martensitic transformation of highly undercooled Ni–Fe–Ga magnetic shape memory alloys

H.X. Zheng, M.X. Xia, J. Liu, J.G. Li*

School of Materials Science and Engineering, Shanghai Jiao Tong University, 1954 Huashan Road, Shanghai 200030, PR China

Received 14 June 2004; received in revised form 13 July 2004; accepted 26 July 2004

Abstract

Ni–Fe–Ga alloys were highly undercooled by using molten glass purifier and superheating cycle. Effects of the undercooling on the temperatures of martensitic transformation, microstructures and phase structures were investigated. Compared with the as-melted alloy, there is little effect of the undercooling on the temperatures of the martensitic transformation and the undercooled $Ni_{56}Fe_{17}Ga_{27}$ alloy retained the 14M martensitic structure within the achieved undercooling range of 0–200 K, while in the $Ni_{60}Fe_{17.5}Ga_{22.5}$ alloy, the γ phase formed as primary phase during the stage of rapid solicitation, in addition, the γ phase became more refined and the volume fraction increased up to 76% under the undercooling of 220 K.

Keywords: Ni–Fe–Ga; Martensitic transformation; Magnetic shape memory alloy; High undercooling

1. Introduction

Heusler Ni–Mn–Ga alloys have attracted much attention for potential applications as promising actuators driven by an applied magnetic field [1]. Several new Heusler alloys, such as Ni–Fe–Ga, Co–Ni–Ga, Ni–Mn–Fe–Ga, Co–Ni–Al were developed [2–7]. Extensive investigations have concentrated on single crystals and as-melted polycrystalline alloys [8–11]. Recently, some reports about directional solidified and melt-spun Ni–Mn–Ga alloys have appeared [12,13]. For most Heusler alloys, the conventional synthesis is arc-melting followed by annealing at a specific temperature to achieve a structural transition from B2 to $L2_1$. However, sometimes such a method does not lead to the pure β phase (B2 structure). Once the γ phase is formed, it obstructs the formation of the pure β phase. Melt-spinning can promote the formation of the β phase and impede γ phase formation by enforcing a rapid cooling of the liquid state directly into the pure β phase, that is to say, it can broaden the composition range of the pure $L2_1$ phase effectively. On the other hand, from the viewpoint of magnetic properties, as-spun Ni–Mn–Ga materials have also shown many special magnetic phenomena different from as-melted alloys [13]. High undercooling and melt-spinning both belong to the rapid solidification category [14–16], and competitive nucleation of different phases may occur in undercooled melts. Furthermore, a highly ⟨1 0 0⟩ textured Fe–20 at.% Ga magnetostrictive alloy had been prepared successfully using high undercooling directional crystal growth technique [17]. So, it is rather attractive and necessary to investigate this kind of undercooled magnetic materials. In this article, we undercooled Ni–Fe–Ga magnetic shape memory alloys and reported the initial results of the temperatures of martensitic transformation, microstructures and phase structures under different nucleation conditions.

2. Experimental

Starting materials of $Ni_{56}Fe_{17}Ga_{27}$ and $Ni_{60}Fe_{17.5}Ga_{22.5}$ alloys about 35 g were made by using arc-melting under argon atmosphere (the purity of the elements is higher than 99.99%). The alloys were melted four times to ensure homogeneity. The obtained ingots were cut into 6 mm × 6 mm

* Corresponding author. Tel.: +86-21-62932569; fax: +86-21-62933074.
E-mail address: jywxws@sjtu.edu.cn (J.G. Li).

0925-8388/$ – see front matter © 2004 Elsevier B.V. All rights reserved.
doi:10.1016/j.jallcom.2004.07.028

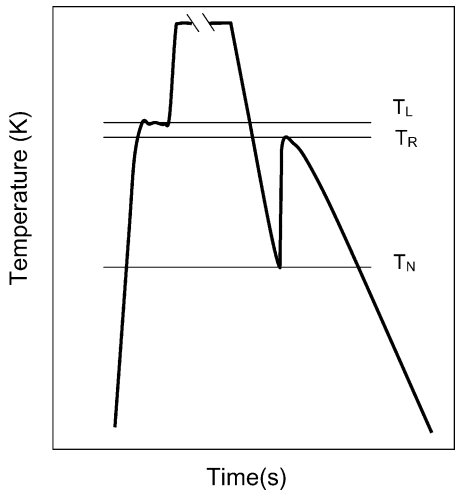

Fig. 1. A typical cooling curve of undercooled $Ni_{56}Fe_{17}Ga_{27}$ alloy.

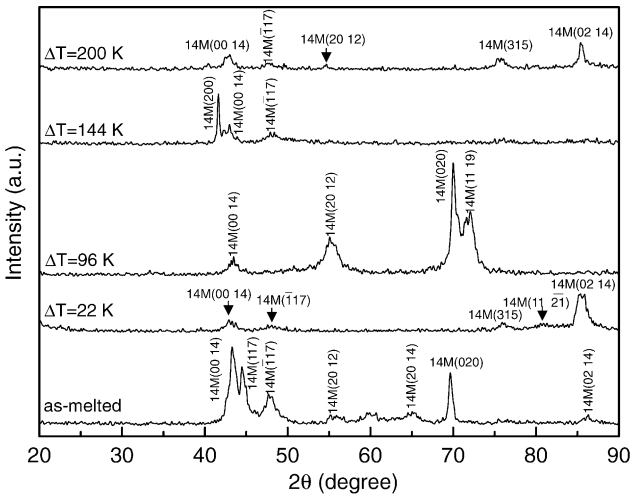

Fig. 3. XRD patterns of $Ni_{56}Fe_{17}Ga_{27}$ alloy at room temperature.

$\times$ 6 mm pieces for use in the following undercooling experiments. The undercooling experiments were performed on a high frequency induction heating unit. To protect the alloy from oxidization and remove inclusion from the melt, a melt-fluxing technique was adopted [16]. The glass purifier, consisting of 50% B_2O_3, 30% Na_2SiO_3 and 20% $Na_2B_4O_7$, was made from the analytical reagents and had been dehydrated by keeping under a molten state at 1173 K for 12 h in advance. Firstly, high purity argon was backfilled into the chamber three times after the vacuum system was evacuated to 2×10^{-3} Pa, and the argon pressure in the chamber was 0.08 MPa. Secondly, the glass purifier and a piece of Ni–Fe–Ga alloy were put into a clean quartz tube and induction heated into liquid for 2 min, then cooled and heated cyclically till the predetermined undercooling was obtained. The overheating temperature was about 200 K. The cooling curve of the melts was measured by an infrared pyrometer, which was calibrated with a standard $PtRh_{30}$–$PtRh_6$ thermocouple, and possessed a relative accuracy of 5 K and a response time less than 1 ms. The obtained undercooled samples were sealed in a vacuum silica tube, heated to 773 K and then cooled slowly to room temperature.

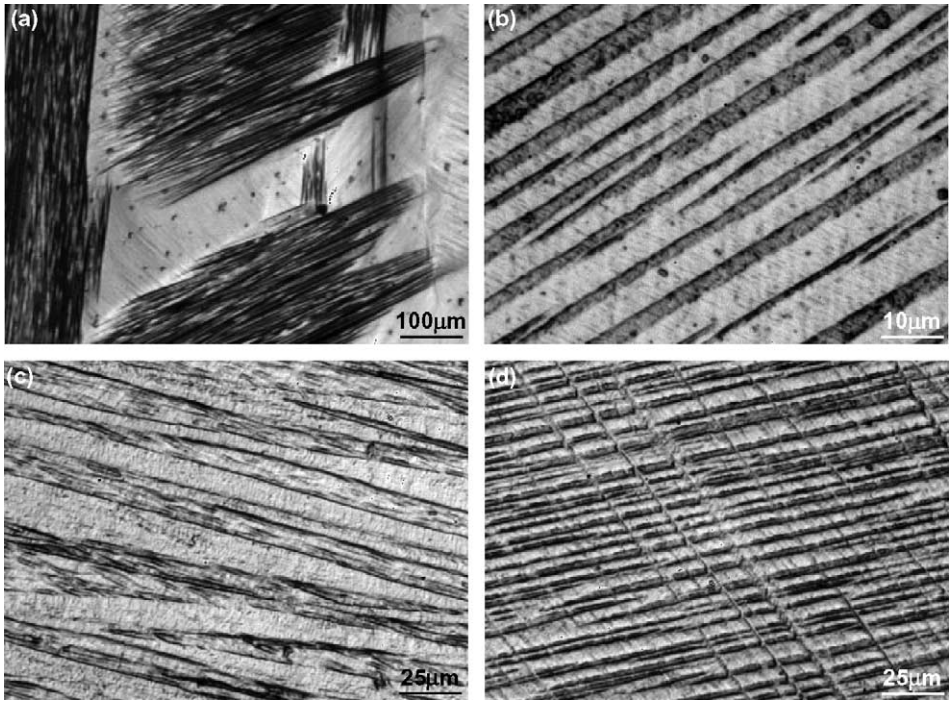

Fig. 2. Microstructures of $Ni_{56}Fe_{17}Ga_{27}$ alloys (a) as-melted, (b) ΔT=22 K, (c) ΔT = 96 K and (d) ΔT = 200 K. (ΔT stands for the undercooling, $\Delta T = T_L - T_N$).

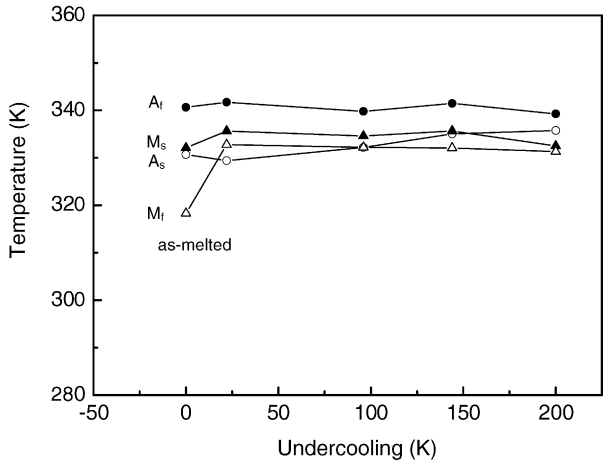

Fig. 4. Martensitic transformation temperatures under different undercoolings of $Ni_{56}Fe_{17}Ga_{27}$ alloy.

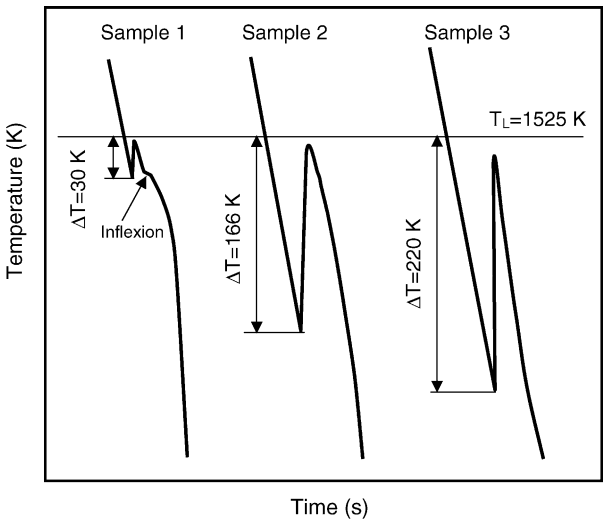

Fig. 5. Cooling curves of undercooled $Ni_{60}Fe_{17.5}Ga_{22.5}$ alloy.

Microstructure observation was carried out using an optical microscope (Neoplot-1) and a scanning electron microscope (SEM520) with EDS. The alloy melting point was measured in a differential thermal analysis (DTA1600). The temperatures of martensitic transformation were measured by a modulated differential scanning calorimeter (MDSC2910) with heating and cooling rates of 5 K/min. Phase identifications were performed by a D8 ADVANCE X-ray power diffractometer with CuK_α radiation.

3. Results and discussion

3.1. $Ni_{56}Fe_{17}Ga_{27}$ alloy

Fig. 1 is a typical cooling curve of undercooled $Ni_{56}Fe_{17}Ga_{27}$ alloy melts. When the melt was undercooled to the nucleation temperature, T_N, nucleation abruptly and growth occurred. Because the solid phase released latent heat the temperature rose quickly to T_R. After this recalescence, the sample cooled down slowly. The notation, T_L, stands for the alloy melting point, 1527 K.

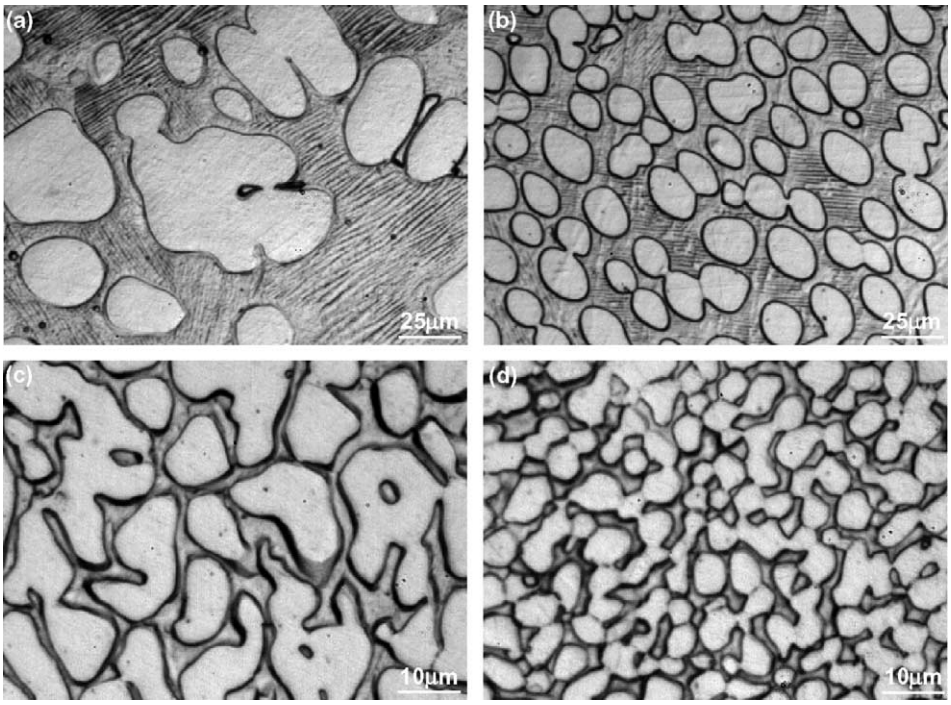

Fig. 6. Microstructures of $Ni_{60}Fe_{17.5}Ga_{22.5}$ alloy, (a) as-melted, (b) ΔT = 30 K, (c) ΔT = 166 K and (d) ΔT = 220 K.

Fig. 2 shows the stripe-like martensitic microstructures of undercooled $Ni_{56}Fe_{17}Ga_{27}$ alloy and no γ phase was found. Fig. 3 are the XRD patterns, which are well identified as 14M martensitic structures and no γ peak was observed, that is, the undercooled $Ni_{56}Fe_{17}Ga_{27}$ alloy retained the initial structure of the as-melted alloy. According to the microstructural evolution, we can conclude that the β phase had formed during the stage of rapid solidification.

The relationship between the temperatures of martensitic transformation and the undercooling is given in Fig. 4. There is almost no change of the temperatures of the martensitic transformation under different degrees of undercooling, which means that the temperatures of martensitic transformation are stable along the growth direction in the directional crystal obtained by using high undercooling directional crystal growth technique and this may be favorable in the practical engineering field.

3.2. $Ni_{60}Fe_{17.5}Ga_{22.5}$ alloy

Fig. 5 shows the cooling curves of $Ni_{60}Fe_{17.5}Ga_{22.5}$ alloy. There was an inflexion in the cooling curve of sample 1 and the inflexion diminished in the cooling curves of samples 2 and 3. From the cooling curves, one can see that the cooling rate increased with increasing undercooling, which means that the residual liquid phase decreased after rapid solidification.

Based on the microstructures (Fig. 6), it is obvious that the γ phase acted as the primary phase and formed during the stage of rapid solidification. The volume fraction of the γ phase increased generally and accounted for 76% under an undercooling of 220 K (Fig. 7), which is in accordance with the XRD patterns (Fig. 8). When the undercooling exceeded 166 K, the peak of the martensitic phase can no longer be clearly observed. In addition, the γ phase became more refined.

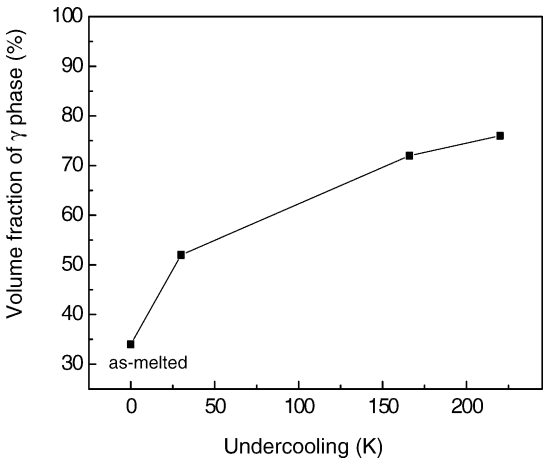

Fig. 7. Volume fraction of γ phase under different undercoolings of $Ni_{60}Fe_{17.5}Ga_{22.5}$ alloy.

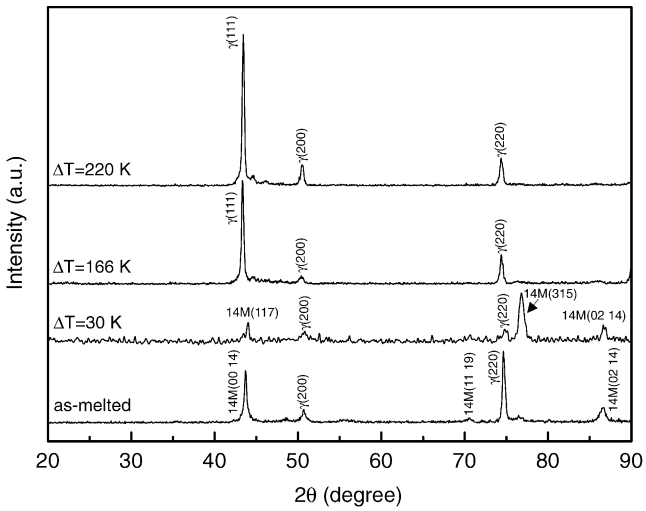

Fig. 8. XRD patterns of $Ni_{60}Fe_{17.5}Ga_{22.5}$ alloy at room temperature.

3.3. Competitive nucleation in undercooled Ni–Fe–Ga melts

Although high undercooling and melt-spinning both can promote fast crystal growth, the essential difference is the driving force of the crystal growth. For the melt-spun alloys, the driving force is dynamic undercooling. Liu et al. [13] prepared pure $L2_1$ phase by melt-spinning and under a high cooling rate, the γ phase was suppressed and the β phase formed directly from the melt. For the undercooled melts, the driving force is thermodynamic undercooling. For different degrees of undercooling, different phases may form during the stage of rapid solidification [15,16]. In this article, within the achieved undercooling range, the β phase is the primary phase in $Ni_{56}Fe_{17}Ga_{27}$ alloy and the γ phase is the primary phase in $Ni_{60}Fe_{17.5}Ga_{22.5}$ alloy. In addition, the glass purifier is very effective to denucleate the Ni–Fe–Ga alloys to obtain a high undercooling. It is possible to prepare a directionally solidified crystal using high undercooling technique provided the proper alloy is chosen. However, up to date, the origin of the competitive nucleation behavior of β and γ phases in undercooled Ni–Fe–Ga alloy melts is still unclear due to insufficient information on the ternary phase diagram, so in future work, more experiments are needed.

4. Conclusions

Ni–Fe–Ga alloys were highly undercooled by using a molten glass purifier and superheating cycle. There is little effect of the undercooling on the temperatures of martensitic transformation and the undercooled $Ni_{56}Fe_{17}Ga_{27}$ alloy retained the 14M martensitic structure within the achieved undercooling range of 0 to 200 K. In the $Ni_{60}Fe_{17.5}Ga_{22.5}$ alloy, the γ phase formed as primary phase and the γ phase refined and the volume fraction increased up to 76% under an undercooling of 220 K.

Acknowledgements

The authors express their appreciation for the financial support of the National Natural Science Foundation and the National Science Fund for Distinguished Scholars of China.

References

[1] K. Ullakko, J. Mater. Eng. Perf. 5 (1996) 405–409.
[2] K. Oikawa, T. Ota, F. Gejima, T. Ohmori, R. Kaimuma, K. Ishida, Mater. Trans. 42 (2001) 2472–2475.
[3] I. Karaman, H.E. Karaca, D.C. Lagoudas, H.J. Maier, Y.I. Chumlyakov, Scr. Mater. 49 (2003) 831–836.
[4] K. Oikawa, T. Ota, Y. Sutou, T. Ohmori, R. Kainuma, K. Ishida, Mater. Trans. 43 (2002) 2360–2362.
[5] A.A. Cherechukin, V.V. Khovailo, R.V. Koposov, E.P. Krasnoperov, T. Takagi, J. Tani, J. Magn. Magn. Mater. 258–289 (2003) 523–525.
[6] H.X. Zheng, M.X. Xia, J. Liu, J.G. Li, J. Alloys Compd. 385 (2004) 144–147.
[7] H.X. Zheng, J. Liu, M.X. Xia, J.G. Li, Martensitic transformation of Ni–Fe–Ga–(Co, Ag) magnetic shape memory alloys, J. Alloys Compd. 387 (2004) 265–268.
[8] O. Heczko, N. Glavatska, V. Gavriljuk, K. Ullakko, Mater. Sci. Forum 373–376 (2001) 341–344.
[9] K. Ullakko, J.K. Huang, V.V. Kokorin, R.C. O'Handley, Scr. Mater. 36 (1997) 1133–1138.
[10] V.A. Chernenko, V. L'vov, J. Pons, E. Cesari, J. Appl. Phys. 93 (2003) 2394–2399.
[11] N.I. Glavatska, A.A. Rudenko, V.A. L'vov, J. Magn. Magn. Mater. 241 (2002) 287–291.
[12] T. Liang, C.B. Jiang, H.B. Xu, Z.H. Liu, M. Zhang, Y.T. Cui, G.H. Wu, J. Magn. Magn. Mater. 268 (2004) 29–32.
[13] Z.H. Liu, M. Zhang, Y.T. Cui, Y.Q. Zhou, W.H. Wang, G.H. Wu, X.X. Zhang, G. Xiao, Appl. Phys. Lett. 82 (2003) 424–426.
[14] D.L. Li, G.C. Yang, Y.H. Zhou, J. Mater. Sci. Lett. 11 (1992) 1033–1035.
[15] D.M. Herlach, J. Gao, D. Holland-Moritz, T. Volkmann, Mater. Sci. Eng. A 375–377 (2004) 9–15.
[16] H.X. Zheng, W.Z. Ma, C.S. Zheng, X.F. Guo, J.G. Li, Mater. Sci. Eng. A 355 (2003) 7–13.
[17] W.Z. Ma, H.X. Zheng, M.X. Xia, J.G. Li, J. Alloys Compd. 379 (2004) 188–192.